Exendin-4 Improves β-Cell Function in Autophagy-Deficient β-Cells

Hiroko Abe, Toyoyoshi Uchida, Akemi Hara, Hiroki Mizukami, Koji Komiya, Masato Koike, Nayumi Shigihara, Yukiko Toyofuku, Takeshi Ogihara, Yasuo Uchiyama, Soroku Yagihashi, Yoshio Fujitani, and Hirotaka Watada

Department of Metabolism and Endocrinology (H.A., T.U., A.H., K.K., N.S., Y.T., T.O., Y.F., H.W.), Center for β-Cell Biology and Regeneration (A.H., Y.F., H.W.), Center for Therapeutic Innovations in Diabetes (H.W.), Center for Molecular Diabetology (H.W.), Sportology Center (H.W.), Department of Cell Biology and Neuroscience (M.K., Y.U.), Juntendo University Graduate School of Medicine, Tokyo, Japan; Department of Pathology and Molecular Medicine (H.M., S.Y.), Hirosaki University Graduate School of Medicine, Hirosaki, Japan; and Japan Science Technology Agency (JST)-CREST Program (Y.F.)

Autophagy is cellular machinery for maintenance of β-cell function and mass. The implication of autophagy failure in β-cells on the pathophysiology of type 2 diabetes and its relation to the effect of treatment of diabetes remains elusive. Here, we found increased expression of p62 in islets of *db/db* mice and patients with type 2 diabetes mellitus. Treatment with exendin-4, a glucagon like peptide-1 receptor agonist, improved glucose tolerance in *db/db* mice without significant changes in p62 expression in β-cells. Also in β-cell-specific Atg7-deficient mice, exendin-4 efficiently improved blood glucose level and glucose tolerance mainly by enhanced insulin secretion. In addition, we found that exendin-4 reduced apoptotic cell death and increased proliferating cells in the Atg7-deficient islets, and that exendin-4 counteracted thapsigargin-induced cell death of isolated islets augmented by autophagy deficiency. Our results suggest the potential involvement of reduced autophagy in β-cell dysfunction in type 2 diabetes. Without altering the autophagic state in β-cells, exendin-4 improves glucose tolerance associated with autophagy deficiency in β-cells. This is mainly achieved through augmentation of insulin secretion. In addition, exendin-4 prevents apoptosis and increases the proliferation of β-cells associated with autophagy deficiency, also without altering the autophagic machinery in β-cells. **(*Endocrinology* 154: 4512–4524, 2013)**

Progressive decreases in pancreatic β-cell function and mass are features of type 2 diabetes mellitus and major determinants of metabolic abnormality in this disorder (1, 2). Thus, understanding the molecular mechanism of these defects seems important in the race to find new therapies for type 2 diabetes.

Autophagy is an intracellular process that involves the rearrangement of subcellular membranes to sequester cytoplasm and organelles for delivery to the lysosomes, where they are degraded and recycled (3). Because autophagy is important for the maintenance of quality of proteins, its impairment results in structural and functional abnormalities in various cells (4–7). Recently, we and others investigated the effects of autophagy deficiency on the morphology and function of β-cells using mice deficient in Atg7, an essential gene for autophagosome formation, specifically in β-cells ($Atg7^{\Delta\beta\text{-cell}}$) (8–10). Morphologic analysis of the pancreas of $Atg7^{\Delta\beta\text{-cell}}$ mice showed accumulation of ubiquitinated proteins, swollen mitochondria, and dilated endoplasmic reticulum (ER) in β-cells. In addition, $Atg7^{\Delta\beta\text{-cells}}$ showed reduced glucose-stimulated insulin secretion with reduced glucose-induced ATP production and increased number of apoptotic cells in islets. These molecular and cellular changes were asso-

ISSN Print 0013-7227 ISSN Online 1945-7170
Printed in U.S.A.

Received June 24, 2013. Accepted October 3, 2013.
First Published Online October 8, 2013

Abbreviations: ATF4, activating transcription factor 4; BMI, body mass index; CHOP, C/EBP homologous protein; ER, endoplasmic reticulum; GFP, green fluorescent protein; GLP-1, glucagon like peptide -1; IPGTT, ip glucose tolerance test; ITT, insulin tolerance test; LC3, microtubule-associated protein 1 light chain 3; RIP-Cre, rat insulin promoter-driven cre-recombinase; SNAP, synaptosomal-associated protein; TUNEL, terminal deoxynucleotide transferase-mediated dUTP nick-end labeling; UPR, unfolded protein response.

ciated with overt hyperglycemia and reduced insulin secretion in Atg7$^{\Delta\beta\text{-cell}}$ mice, indicating that autophagy is important for the maintenance of structure and function of β-cells (8–10). Atg7$^{\Delta\beta\text{-cell}}$ mice also showed enhanced β-cell apoptosis under a insulin resistance state induced by high-fat diet. The resultant inadequate expansion of β-cells seemed to result in further deterioration of glucose tolerance in Atg7$^{\Delta\beta\text{-cell}}$ mice under insulin resistance (8). This phenotype is similar to defective β-cells observed in type 2 diabetes mellitus, suggesting the pathologic role of failure of β-cell autophagy in β-cell dysfunction in type 2 diabetes mellitus. At this stage, however, the role of autophagy failure of β-cells in the pathophysiology of type 2 diabetes and its relation to the outcome of treatment remains elusive.

Glucagon-like peptide-1 (GLP-1) receptor agonists, such as exendin-4, are effective agents for type 2 diabetes mellitus (11–13) and enhance glucose-induced insulin secretion while preserving β-cell mass by stimulating β-cell proliferation and inhibiting β-cell apoptosis (14–16). However, the effects of GLP-1 receptor agonists on β-cell dysfunction associated with autophagy failure remain to be determined.

The present study focused on the following 2 important questions: 1) is failure of autophagy related to β-cell dysfunction in type 2 diabetes? To answer this question, we measured the level of p62 in islets in a mouse model of type 2 diabetes and autopsy samples from patients with type 2 diabetes; and 2) can exendin-4 improve β-cell dysfunction and apoptotic β-cell death induced by autophagy failure? The second part of the study examined the effect of exendin-4 in Atg7$^{\Delta\beta\text{-cell}}$ mice.

Materials and Methods

Immunohistochemical analysis of human samples

The study protocol using human samples was approved by the ethics review committees of Hirosaki University. From the archival files of autopsy cases at Hirosaki University and its affiliated teaching hospitals, pancreatic tissues were collected from 24 consecutive persons with diabetes and 15 age-, sex-, and body mass index (BMI)-matched control cases that had no history of diabetes. The tissue samples were fixed in 10% buffered formalin and stored in paraffin. Sections were obtained from these tissue blocks for hematoxylin-eosin staining and immunohistochemistry. Immunohistochemical staining was conducted by the avidin-biotin-peroxidase complex method. Briefly, 4-μm-thick deparaffinized sections were immersed in Tris-buffered saline and placed in pressure chamber (Pascal, Dako Cytomation) for antigen retrieval (121°C, 1 minute in Tris-EDTA buffer). To eliminate endogenous peroxidase activity, the sections were pretreated with background sniper (Biocare Medical) for 10 minutes at room temperature. Then the sections were incubated with the first antibody against p62 (clone 5F-2, 1:50, mouse monoclonal; Medical & Biological Laboratory Co.). The immunoreaction products were colorized with diaminobenzidine. The specificity of any positive results was confirmed by negative staining following omission or replacement of the first antibody with nonimmune mice sera. By counting more than 40 000 islet cells per case, the proportion of p62-positive endocrine cells per the entire population of endocrine cells in islets was calculated. This analysis was performed by investigators blinded to the clinical information.

Double immunofluorescence was applied to confirm the coexpression of insulin and P62. The primary antibodies for insulin (guinea pig polyclonal, 1:250; Dako Cytomation) and P62 were simultaneously applied to pancreas sections, followed by incubation with a cocktail of Alexa-fluor 594-conjugated antimouse secondary antibody (dilution, 1:1000; Invitrogen) and Alexa-fluor 488-conjugated antiguinea pig secondary antibody (dilution, 1:1000; Invitrogen) for 30 minutes at room temperature. Subsequently, insulin-positive β-cells were identified as green whereas P62-positive cells appeared red on a fluorescent microscope (Axioimager M1, Carl Zeiss Co).

Mice

The study protocol of animal experiments was approved by the ethics review committees of Juntendo University. All mice were housed in specific pathogen-free barrier facilities, maintained under a 12-hour light, 12-hour dark cycle, and fed a standard rodent food (Oriental Yeast Co.) or rodent food containing 60% fat (D12492, Research Diet) and water ad libitum. The approximate fatty acid profile of the high-fat diet is 32% saturated, 36% monounsaturated, and 32% polyunsaturated. Male C57BL6/J, db/misty (*db/m*) and *db/db* mice on a C57BL6/J background were obtained from CLEA Japan Inc. We used the rat insulin promoter-driven cre-recombinase (RIP-Cre) to delete the *ATG7* gene in a pancreatic β-cell-specific manner. The generation of Atg7flox/+ mice was described previously (5). RIP-Cre$^{+/-}$:Atg7flox/flox mice were crossed with Atg7flox/flox mice to generate Atg7flox/flox (Atg7$^{f/f}$) and RIP-Cre$^{+/-}$:Atg7flox/flox (Atg7$^{\Delta\beta\text{-cell}}$) mice.

To assess the acute effects of exendin-4 on glucose tolerance and insulin secretion, 8-week-old Atg7$^{f/f}$ andAtg7$^{\Delta}$β-cell mice were injected ip with exendin-4 (Sigma-Aldrich) at 24 nmoL/kg body weight or volume-matched saline at 30 minutes before glucose challenge. To assess the chronic effects of exendin-4, exendin-4 was infused continuously at 24 nmoL/kg body weight/d, or volume-matched saline in control mice, using a miniosmotic pump (ALZEST, model 1004; DURECT), which delivers the solution for up to 28 days, from the age of 8 to 12 weeks in Atg7$^{f/f}$ and Atg7$^{\Delta}$β-cell mice, and from the age of 6 to 10 weeks in db/misty and *db/db* mice.

Measurement of blood glucose and insulin levels

Random blood glucose level was measured between 10:00 AM and 12:00 AM under ad libitum feeding condition using blood samples obtained from the tail vein. Between the age of 8 and 12 weeks, after an overnight fasting, mice were injected with glucose at 1.0 g/kg for ip glucose tolerant test (IPGTT), and 2.0 U/kg insulin for insulin tolerance test (ITT), respectively, as described in detail previously (17). Glucose levels were measured using a glucose analyzer (Free Style, KISSEI Pharma Co) at the indicated

time points, whereas insulin levels were measured by ELISA kit (Morinaga Co).

Assays using isolated islets and pancreas

Pancreatic islets were isolated by collagenase digestion, as described previously (17), after which 5 size-matched islets were incubated in 400 μL Krebs Ringer buffer containing 2.8 or 16.7 mM glucose to assess insulin secretion. To measure whole pancreas insulin content, whole pancreas was solubilized in an acid-ethanol solution overnight at 4°C, after which the samples were analyzed by an ELISA kit for measurement of insulin content (Morinaga Co.). To measure ATP content, the isolated islets were incubated in Krebs Ringer buffer with 2.8 or 16.7 mM glucose for 30 minutes (8). The incubation was terminated by adding 30% trichloroacetic acid (final 5%), followed by sonication. After centrifugation (2000 × *g* for 3 minutes), the supernatant (0.9 mL) was mixed with 1.0 mL water-saturated diethyl ether, and the ether phase containing trichloroacetic acid was discarded. This procedure was repeated 4 times. The final aliquot (0.4 mL) was diluted with 0.1 mL 40 mM HEPES (pH 7.4). ATP contents were assayed by applied luciferase reaction using the ATP assay system LL-100–1 (Toyo Inc). The emission was measured by luminometer Lumat LB9507 (EG6G Berthold).

Establishment of inducible Atg7 knockdown INS-1 cells (Atg7KD INS-1)

To establish cells overexpressing Tet repressor that allows tetracycline-regulated expression of the gene of interest in mammalian cells, we used pT-REx-DEST Gateway Vectors (Invitrogen). Micro-RNA of ATG7 gene was inserted into pcDNA6.2-GW/EmGFP-miR (Invitrogen) to obtain micro-RNA combined with a green fluorescent protein (GFP) construct. The combination was then inserted into the specific donor vector (pDONR211). Next, pDONR211 was recombined into pT-REx system plasmid (pT-REx-DEST30). Finally, pT-REx-DEST30-ATG7-miR-GFP and repressor (pcDNA6/TR) were cotransfected into INS-1 cells using the transfection agent, Effectene (QIAGEN). Several clones were isolated after the selection using Blasticidin-S (for pcDNA6/TR) and G418 (for pT-REx-DEST30). We chose tetracycline-inducible Atg7 knock down INS-1 cells (Atg7KD INS-1), based on their high knockdown efficiency. We also generated control INS-1 cells (Atg7WT INS-1) without knockdown activities.

Assay of islets and Atg7KD INS-1 cells death

Twenty size-matched islets were placed on Millicell culture plate inserts (Millipore) and incubated with exendin-4 or NaCl. After a 15-hour incubation, the islets were treated with thapsigargin (Sigma,) or dimethylsulfoxide, as described previously (18). Atg7KD INS-1 and Atg7WT INS-1 were plated on 96-well plates. After 24 hours culture, these cells were incubated with 2 μg/mL tetracycline and with exendin-4 or NaCl. After another 72 hours, these cells were treated with thapsigargin or dimethylsulfoxide for 4 hours. To assess cell death, we determined oligonucleosomes released in cultured cell lysate by using Roche ELISA kit.

Immunohistochemical analysis and quantification of β-cell area

Immunohistochemistry was applied for measurement of the relative area of β-cells in the pancreas using the method described previously (19). The following primary antibodies were used: guinea pig antihuman insulin antibody (Linco Research), chicken antihuman insulin antibody (Abcam), guinea pig anti-p62 antibody (PROGEN), rabbit anticleaved caspase-3 antibody (Cell Signaling Technology), and mouse antihuman Ki67 Ab (BD Biosciences). For terminal deoxynucleotide transferase-mediated dUTP nick-end labeling (TUNEL) assay, in situ Apoptosis Detection kit (TKR) was used. Sections were counterstained with methylene blue. β-Cell mass and number of intraislet cells positive for cleaved caspase-3, Ki67, or TUNEL were determined, as described previously (8).

Electron microscopy

Each mouse was anesthetized with pentobarbital sodium, and the pancreas was removed after cardiac perfusion and then fixed in a solution of 2.5% glutaraldehyde. The samples were cut into pieces, block stained with 1% aqueous solution of uranyl acetate, dehydrated with graded series of ethanol, and embedded in Epon 812 (TAAB Laboratories Equipment). Ultrathin sections were cut with a Leica Ultracut UCT (Leica), stained with uranyl acetate and lead citrate, and observed under a JEM-1230EX electron microscope (EM) (JEOL) operated at 80 kV.

Tissue RNA isolation and quantitative RT-PCR

Total RNA from approximately 200 islets harvested from all mice was isolated using QIAshredder and RNeasy Plus Micro Kit (QIAGEN). The first-strand cDNA was synthesized using 0.3 μg of total RNA with random primers and Superscript reverse transcriptase (Invitrogen, Life Technologies Corp.). For quantitative SYBR Green real-time PCR, cDNA was analyzed by ABI 7500 Fast Real-Time PCR System with SYBR Green PCR Master Mix (Applied Biosystems, Life Technologies Corp.) and specific primers. The thermal cycle for amplification was set as follows; 20 seconds at 95°C and 40 cycles of 95°C for 3 seconds and 60°C for 30 seconds. Using this protocol, neither nonspecific primer-dimer amplification nor PCR products were observed in no-template control samples. Single-band PCR products were detected by 2% agarose gels with end-reaction products. The relative mRNA expression level was analyzed using the standard curve method. As an internal invariant standard, we used TATA box-binding protein mRNA.

Immunoblot analysis

Immunoblot analysis using islet cell extracts was performed as described previously (8). Anti-microtubule-associated protein-1 light chain 3 (LC3) antibody was obtained from Sigma Aldrich, p62 from PROGEN, Bip from BD Biosciences, p-PERK, PERK, p-eIF2α, eIF2α, and glyceraldehyde 3-phosphate dehydrogenase from Cell signaling Technology, and activating transcription factor 4 (ATF4) and C/EBP homologous protein (CHOP) from Santa Cruz Biotechnology.

Data analysis

Results are presented as mean ±SEM. The Mann-Whitney U test was used for statistical analysis of differences in the number

of p62-positive cells in autopsy samples. Differences in sequential physiologic data of glucose concentration, body weight, food intake, and glucose and insulin levels during IPGTT and ITT were examined for statistical significance using nonrepeated ANOVA with Bonferroni's post hoc test. Statistical differences between 2 groups were calculated by the unpaired Student's *t* test. $P < .05$ denoted the presence of a statistically significant difference.

Results

Accumulation of p62 in pancreatic islets of *db/db* mice and type 2 diabetic patients

To investigate the autophagy state in insulin-resistant and type 2 diabetic mice, we analyzed the expression of LC3 and p62, a specific substrate of autophagy, in islets isolated from C57BL/6 mice fed high-fat diet for 12 weeks and *db/db* mice. As reported previously, mice fed high-fat diet for 12 weeks developed insulin resistance but had near-normal glucose tolerance (data not shown) (8). Six-week old *db/db* mice exhibited insulin resistance and glucose intolerance and showed further deterioration of glucose tolerance at 8 weeks of age (see Figure 2B and data not shown). LC3 type 2 expression was higher in islets of high-fat-fed mice and *db/db* mice than mice fed standard diet and *db/m* mice, respectively (Figure 1A). These results suggest enhanced autophagosome formation in islets of insulin-resistant mice. On the other hand, islets of high-fat-fed mice showed no significant increase in p62 expression, whereas islets of *db/db* mice showed significant increase of p62. Although it was difficult to discriminate β-cells from non-β-cells because of the increased number of degranulated β-cells, immunohistochemical staining confirmed the presence of some p62-expressing insulin-positive cells in *db/db* mice. In contrast, no such p62-positive cells were observed in islets of *db/m* mice (Figure 1B). These results suggest that autophagic turnover is compromised in β-cells of mice with decompensated insulin resistance.

Next, we quantified the number of p62-positive cells in β-cells in human type 2 diabetes. For this purpose, we examined the expression of p62 in the pancreas of 24 diabetic and 15 age-, sex-, and BMI-matched nondiabetic autopsy cases. The mean age, male-female ratio, and mean BMI of the diabetic subjects were 67.2 ± 1.9 years, 18:6, and 23.4 ± 1.0 kg/m^2, respectively, whereas the respective values for the nondiabetic subjects were 64.5 ± 2.7 years, 10:5, 23.5 ± 0.9 kg/m^2. The percentage of p62-positive cells was significantly higher in diabetic (6.1 ± 1.7%) than nondiabetic islet cells (1.1 ± 0.4%) (Figure 1, C and D). In addition, some p62-positive cells costained with insulin (Figure 1E). These results suggest decreased autophagic turnover in β-cells of patients with type 2 diabetes mellitus.

Exendin-4 does not alter p62 expression in *db/db* mice

In this series of experiments, we investigated the effects of GLP-1 receptor agonists on β-cell dysfunction associated with autophagy deficiency. For this purpose, we compared the effects of 4-week exendin-4 treatment in *db/db* and *db/m* mice. During the treatment, significant decrease of random glucose concentration, without significant change in body weight, was observed in both groups of mice. Furthermore, the absolute reduction in blood glucose level of *db/db* mice exceeded that of *db/m* mice (Figure 2, A and B). After the completion of a 4-week treatment, marked and modest improvement of glucose tolerance was observed in both groups of mice, without significant changes in serum insulin level (Figure 2, C–E). Given that serum insulin level in exendin-4-treated *db/db* mice was similar to that in nontreated *db/db* mice (despite the difference in blood glucose level), improvement of β-cell function was considered to play a role, at least in part, in the observed improvement of glucose metabolism induced by exendin-4 in these mice. These findings are compatible with previous data on the effect of GLP-1 receptor agonists in *db/db* mice (20).

In this setting, we then evaluated p62 expression in islets of exendin-4-treated *db/db* mice. As shown in Figure 1B, p62 expression was observed in β and non-β-cells in islets of untreated *db/db* mice. Treatment with exendin-4 did not affect the expression of p62 in both insulin-positive and non-insulin-positive cells. These results suggest that exendin-4 improved β-cell function in *db/db* mice without affecting the autophagic activity of β-cells (Figure 2F).

Exendin-4 improves glucose tolerance in Atg7$^{\Delta}$β-cell mice

To further investigate whether exendin-4 improves β-cell dysfunction associated with autophagy deficiency, we used Atg7$^{\Delta\beta\text{-cell}}$ mice as a model of autophagy failure-induced β-cell dysfunction. First, we compared the effects of a single dose of exendin-4 on glucose tolerance in 12-week-old Atg7$^{\Delta\beta\text{-cell}}$ and Atg7$^{f/f}$ mice. Atg7$^{\Delta\beta\text{-cell}}$ mice exhibited glucose intolerance, but exendin-4 significantly improved their glucose tolerance to levels similar to that in Atg7$^{f/f}$ mice (Figure 3, A and B), and such improvement was accompanied by enhanced insulin secretion (Figure 3C).

We also tested the effects of 4-week treatment with exendin-4 (or saline) in Atg7$^{\Delta\beta\text{-cell}}$ and Atg7$^{f/f}$ mice. During the treatment, each group of mice displayed similar

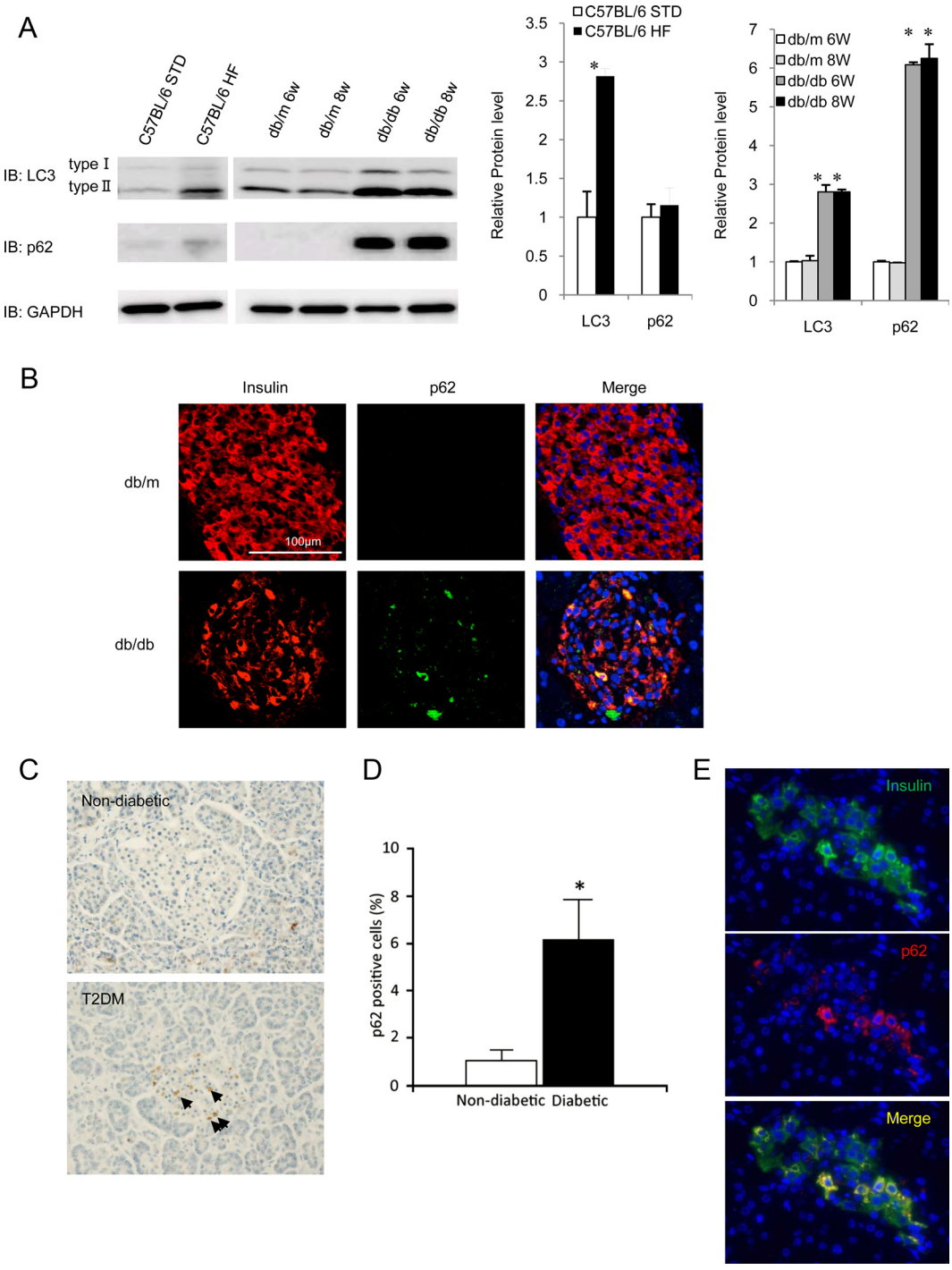

Figure 1. Autophagy in β-cells of mice with insulin resistance and diabetes and also in cadavers of patients with type 2 diabetes A, Pancreatic islets were isolated from C57BL/6 mice fed standard diet (STD) or high-fat diet (HF), db/misty (*db/m*) mice and *db/db* mice at the age of 6 and 8 weeks. Western blotting was performed using LC3 and p62 antibodies. Representative results (left panel) and quantification of protein expression (right panel). Data are mean ± SEM of at least 4 independent experiments. *, $P < .05$, vs C57BL/6STD or *db/m* mice at the corresponding age. B, Representative insulin (red) and P62 (green) staining in *db/m* and *db/db* mice at the age of 10 weeks. C, Representative immunohistochemical staining of p62 using pancreatic specimens from autopsy cases of a nondiabetic subject and diabetic subject (left panel). Accumulation of p62 in islets is marked by the arrow. Magnification, ×20. D, Quantification of p62-positive cells in cadavers of nondiabetic and diabetic subjects. Data are mean ± SEM. *, $P < .05$, between nondiabetics and type 2 diabetic subjects. E, Insulin (green) and p62 (red) staining in an autopsy sample from a representative patient with type 2 diabetes. 6W, 6 weeks; 8W, 8 weeks; GAPDH, glyceraldehyde 3-phosphate dehydrogenase; T2DM, type 2 diabetes mellitus.

weight gain and consumed a similar amount of food (data not shown). Whereas randomly measured blood glucose concentrations of Atg7$^{\Delta\beta\text{-cell}}$ mice were higher than those of Atg7$^{f/f}$ mice, exendin-4 significantly reduced glucose concentration in Atg7$^{\Delta\beta\text{-cell}}$ mice, reaching levels comparable to those of Atg7$^{f/f}$ mice (Figure 3D). After a 4-week-treatment, insulin sensitivity on ITT was comparable among the 4 groups (Figure 3E). IPGTT conducted at the end of treatment showed that exendin-4 had induced marked and modest improvement of glucose tolerance in Atg7$^{\Delta\beta\text{-cell}}$ and Atg7$^{f/f}$ mice, respectively (Figure 3, F and G). Whereas exendin-4 is known to alter insulin response at 30 minutes after glucose injection in Atg7$^{\Delta}\beta$-cell but not in Atg7$^{f/f}$ mice (21) (Figure 3H), the ratio of increment in insulin concentration to that in glucose concentration at 15 minutes after glucose injection indicated that exendin-4 improved early-phase insulin secretion in both Atg7$^{\Delta\beta\text{-cell}}$ and Atg7$^{f/f}$ mice (Figure 3I).

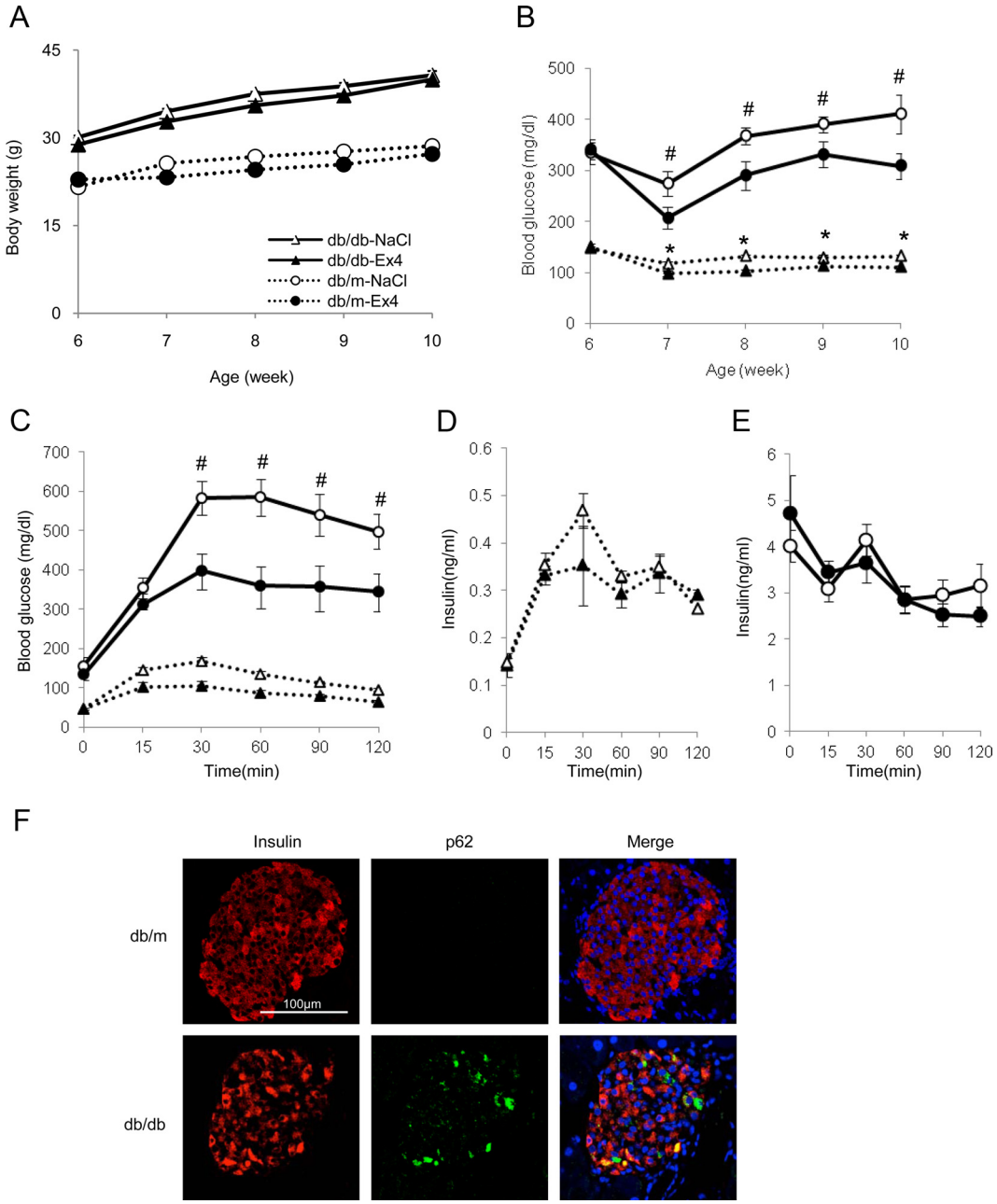

Figure 2. Effects of exendin-4 on *db/m* and *db/db* mice Serial changes in (A) body weight, (B) glucose concentration in random blood samples, and blood glucose level (C) and insulin level (D and E) during IPGTT after exendin-4 or saline treatment for 4 weeks. Open circles, saline-treated *db/db* mice (db/db-NaCl, n = 12); solid circles, exendin-4-treated *db/db* mice (db/db-Ex-4, n = 12); open triangles, saline-treated *db/m* mice (db/m-NaCl, n = 12); solid triangles, exendin-4-treated *db/m* mice (db/m-Ex-4, n = 12). Data are mean ± SEM. *, $P < .05$, db/m-NaCl vs db/m-Ex-4. #, $P < .05$, db/db-NaCl vs db/db-Ex4. F, Representative insulin (red) and P62 (green) staining of *db/m* and *db/db* mice after 4-week treatment with exendin-4.

Furthermore, insulin response in Atg7$^{\Delta\beta\text{-cell}}$ mice during IPGTT was markedly potentiated by exendin-4 (Figure 3, H and I). These results suggest that exendin-4 improves impaired glucose tolerance with decreased insulin secretion in Atg7$^{\Delta\beta\text{-cell}}$ mice.

Four-week treatment with exendin-4 improves glucose-stimulated insulin secretion in Atg7$^{\Delta}$β-cell islets

In the next step, we evaluated the long-term effects of exendin-4 on β-cell function. First, exendin-4 did not alter

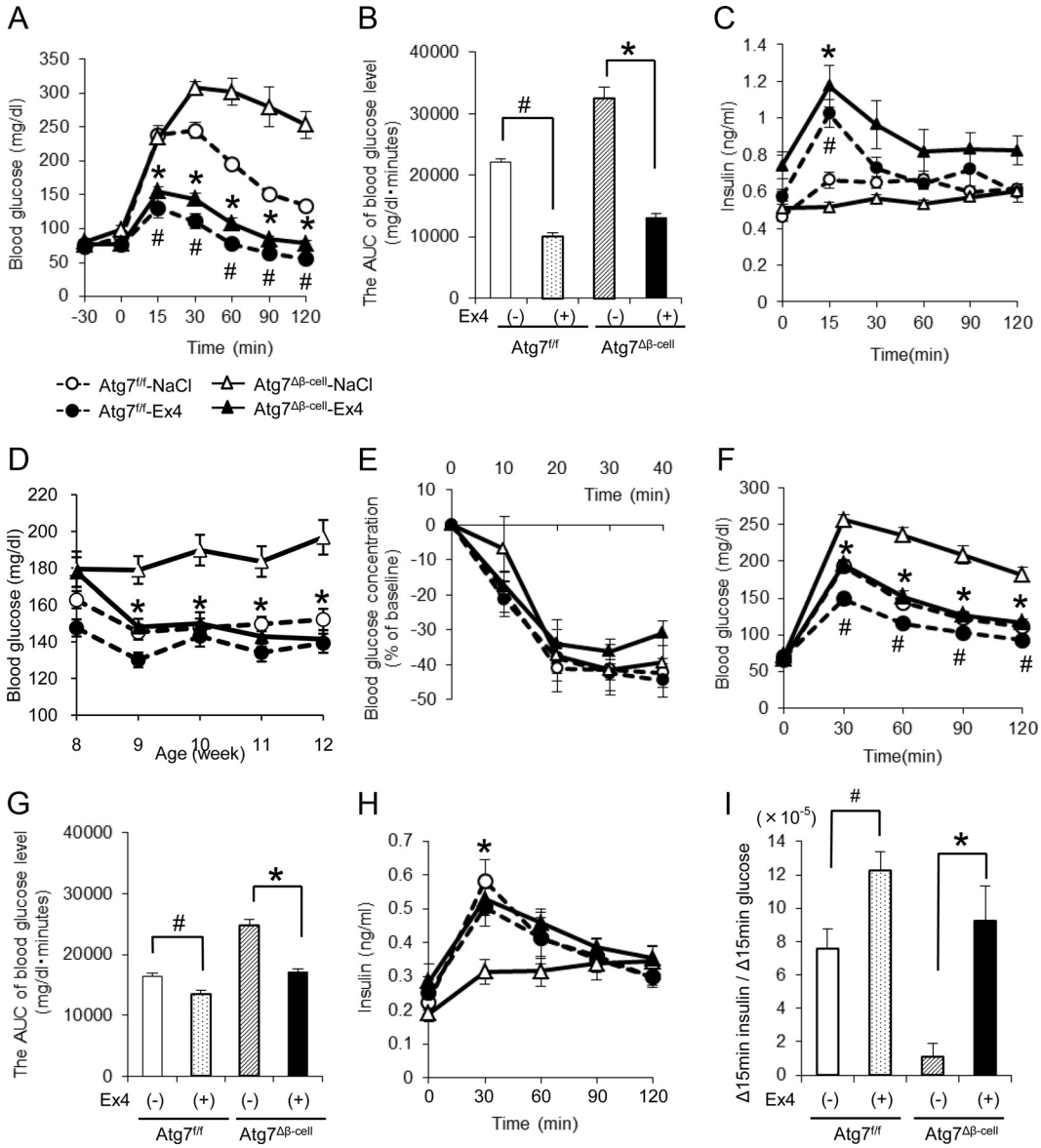

Figure 3. Effects of single injection of exendin-4 and 4-week treatment with exendin-4 on glucose tolerance in Atg7$^{\Delta}$β-cell mice A–C, Blood glucose level (A), area under the curves (AUC) of blood glucose level (B), and insulin level (C) during IPGTT at 30 minutes after ip injection of exendin-4 (24 nmoL/kg body weight) or volume-matched saline in Atg7$^{f/f}$ and Atg7$^{\Delta}$β-cell mice. Open circles and open bars, saline-injected Atg7$^{f/f}$ mice (Atg7$^{f/f}$-NaCl, n = 8); solid circles and dotted bars, exendin-4-injected Atg7$^{f/f}$ mice (Atg7$^{f/f}$-Ex-4, n = 9); open triangles and hatched bars, saline-injected Atg7$^{\Delta}$β-cell mice (Atg7$^{\Delta}$β-cell-NaCl, n = 6); solid triangles and solid bars, exendin-4-injected Atg7$^{\Delta}$β-cell (Atg7$^{\Delta}$β-cell-Ex-4, n = 6). D, Random blood glucose concentrations in Atg7$^{f/f}$ mice and Atg7$^{\Delta}$β-cell mice during 4-week treatment with saline or exendin-4. E Blood glucose concentrations during ITT performed after 4 weeks of continuous infusion of saline or exendin-4. F–H, Blood glucose concentrations (F), the AUC of blood glucose level, and plasma insulin levels (H) during IPGTT performed after 4 weeks of continuous infusion of saline or exendin-4. D–H, Open circles and open bars indicate Atg7$^{f/f}$-NaCl (n = 19); solid circles and dotted bars indicate Atg7$^{f/f}$-Ex4 (n = 20); open triangles and hatched bars indicate Atg7$^{\Delta}$β-cell-NaCl (n = 18); and solid triangles and solid bars indicate Atg7$^{\Delta}$β-cell-Ex4 (n = 20). I, The ratio of increment in insulin concentration to the increment in glucose concentration at 15 minutes during IPGTT. D–H, Open circles and open bars indicate Atg7$^{f/f}$-NaCl (n = 5); solid circles and dotted bars indicate Atg7$^{f/f}$-Ex4 (n = 5); open triangles and hatched bars indicate Atg7$^{\Delta}$β-cell-NaCl (n = 5); and solid triangles and solid bars indicate Atg7$^{\Delta}$β-cell-Ex4 (n = 5). Data are mean ± SEM. *, $P < .05$; Atg7$^{\Delta}$β-cell-NaCl vs Atg7$^{\Delta}$β-cell-Ex4; #, $P < .05$, Atg7$^{f/f}$-NaCl vs Atg7$^{f/f}$-Ex4.

p62 accumulation in islets of Atg7$^{\Delta\beta\text{-cell}}$ cells (Figure 4A). Insulin secretion was assessed by batch incubation after overnight culture of isolated islets in the absence of exendin-4, in order to avoid the residual direct effect of exendin-4. Insulin secretion at low glucose concentration (2.8 mM) was comparable among the groups. However, the secretion under high glucose concentration (16.7 mM) was significantly lower in Atg7$^{\Delta\beta\text{-cell}}$ islets compared with

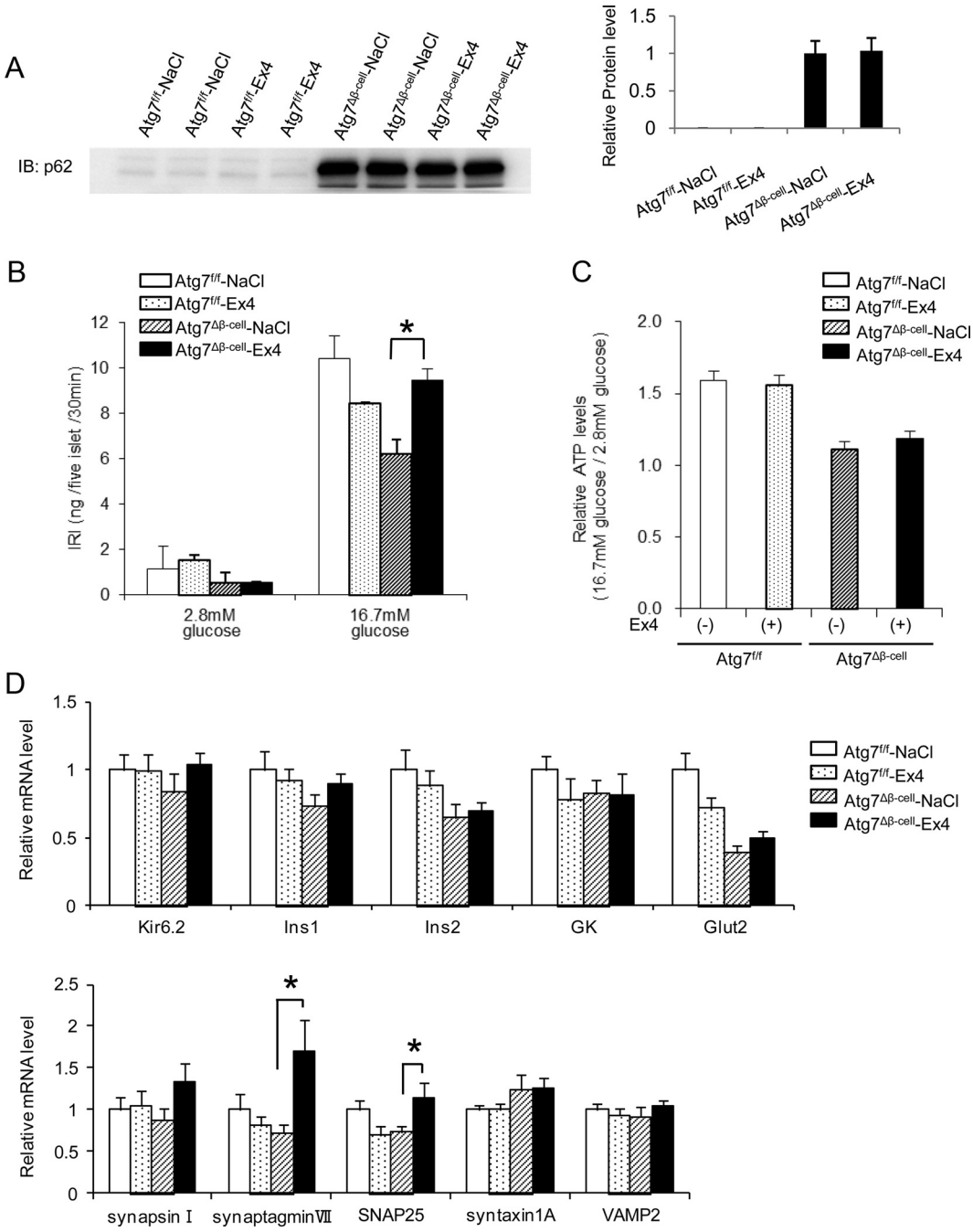

Figure 4. Effects of 4-week treatment with exendin-4 on insulin secretion and gene expression in Atg7$^{\Delta}\beta$-cell islets A, Islets were isolated from Atg7$^{f/f}$-NaCl, Atg7$^{f/f}$-Ex4, Atg7$^{\Delta}\beta$-cell-NaCl, and Atg7$^{\Delta}\beta$-cell-Ex4. Western blotting was performed using p62 antibody. Representative results (left panel) and quantification of protein expression (right panel). Data are mean ± SEM of 4 independent experiments. B, Insulin secretion at the indicated glucose concentrations from islets isolated from Atg7$^{f/f}$-NaCl (open bars, n = 10), Atg7$^{f/f}$-Ex4 (dotted bars, n = 15), Atg7$^{\Delta}\beta$-cell-NaCl (hatched bars, n = 11), and Atg7$^{\Delta}\beta$-cell-Ex4 (solid bars, n = 13). C, Glucose-stimulated ATP production from isolated islets of Atg7$^{f/f}$-NaCl (open bars, n = 9), Atg7$^{f/f}$-Ex4 (dotted bars, n = 6), Atg7$^{\Delta}\beta$-cell-NaCl (hatched bars, n = 6), and Atg7$^{\Delta}\beta$-cell-Ex4 (solid bars, n = 9). Data are presented as fold increase in ATP levels induced by 16.7 mM glucose relative to the levels with 2.8 mM glucose. D, The mRNA expression levels in islets of each group. The mRNA levels were determined by real-time RT-PCR analysis after extraction of RNA from the isolated islets. Data are mean ± SEM. Atg7$^{f/f}$-NaCl (open bars, n = 6), Atg7$^{f/f}$-Ex4 (dotted bars, n = 7), Atg7$^{\Delta}\beta$-cell-NaCl (hatched bars, n = 5), and Atg7$^{\Delta}\beta$-cell-Ex4 (solid bars, n = 4). *, $P < .05$, Atg7$^{\Delta}\beta$-cell-NaCl vs Atg7$^{\Delta}\beta$-cell-Ex4. IB, immunoblotting.

Atg7$^{f/f}$, as reported previously (8) (Figure 4B). Four-week treatment with exendin-4 increased insulin secretion from Atg7$^{\Delta\beta\text{-cell}}$ islets at high glucose concentrations, reaching levels similar to those of Atg7$^{f/f}$ islets.

Next, we investigated the effect of 4-week treatment with exendin-4 on glucose-induced ATP production. Although Atg7$^{\Delta\beta\text{-cell}}$ islets showed diminished glucose-induced ATP production, as reported previously (8), exendin-4 failed to improve glucose-stimulated ATP production in Atg7$^{\Delta\beta\text{-cell}}$ islets (Figure 4C).

To investigate the changes in the expression of genes that are known to be involved in improvement of insulin secretion, we quantitated the mRNA expression of genes important for β-cell function. Among the genes investigated, exendin-4 increased the expression of synaptotagmin VII and synaptosomal-associated protein (SNAP) 25 (Figure 4D).

Exendin-4 treatment prevents apoptotic cell death in Atg7$^{\Delta}$β-cell islets

We have reported previously an increased rate of apoptosis in islets of Atg7$^{\Delta\beta\text{-cell}}$ mice, without significant changes in β-cell mass or proportion of Ki67-positive cells (8). To investigate the effect of exendin-4 on apoptotic cell death, we counted the number of cleaved caspase-3- and TUNEL-positive cells in islets of Atg7$^{\Delta\beta\text{-cell}}$ mice. As shown in Figure 5, A and B, 4-week exendin-4 treatment significantly reduced apoptosis. In addition, the same treatment increased the number of Ki67-positive cells in islets, suggesting increased proliferation of islets of Atg7$^{\Delta\beta\text{-cell}}$ mice (Figure 5C). However, the 4-week treatment did not increase insulin content or β-cell mass in Atg7$^{\Delta\beta\text{-cell}}$ islets (Figure 5, D and E).

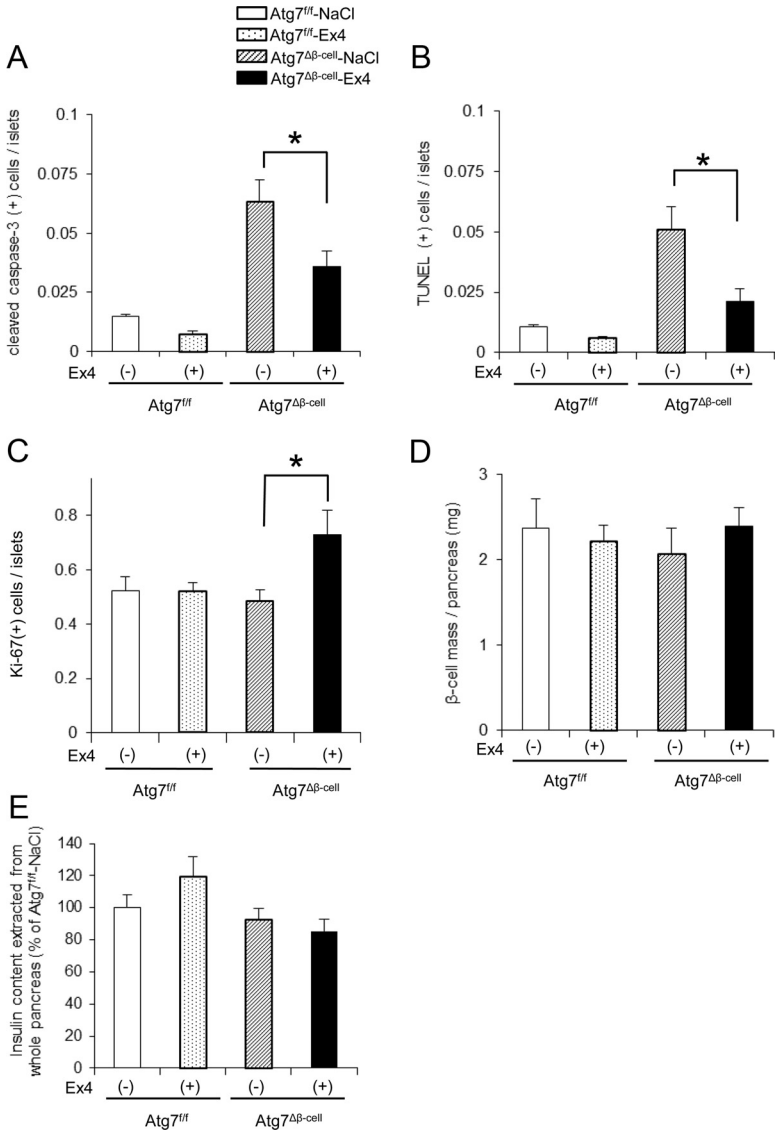

Figure 5. Exendin-4 treatment prevents apoptotic cell death in Atg7$^{\Delta}$β-cell islets Numbers of (A) cleaved caspase-3, (B) TUNEL-positive cells in islets of Atg7$^{f/f}$-NaCl (n = 7), Atg7$^{f/f}$-Ex4 (n = 7), Atg7$^{\Delta}$β-cell-NaCl (n = 6), and Atg7$^{\Delta}$β-cell-Ex4 mice (n = 6). C, Ki67-positive cells in islets of Atg7$^{f/f}$-NaCl (n = 5), Atg7$^{f/f}$-Ex4 (n = 5), Atg7$^{\Delta}$β-cell-NaCl (n = 5), and Atg7$^{\Delta}$β-cell-Ex4 mice (n = 5). D, The calculated β-cell mass in Atg7$^{f/f}$-NaCl (n = 5), Atg7$^{f/f}$-Ex4 (n = 5), Atg7$^{\Delta}$β-cell-NaCl (n = 5), and Atg7$^{\Delta}$β-cell-Ex4 (n = 5) mice. E, Whole pancreas insulin content in Atg7$^{f/f}$-NaCl (n = 7), Atg7$^{f/f}$-Ex4 (n = 9), Atg7$^{\Delta}$β-cell-NaCl (n = 12), and Atg7$^{\Delta}$β-cell-Ex4 (n = 10) mice. Data are mean ± SEM. *, $P < .05$, Atg7$^{\Delta}$β-cell-NaCl vs Atg7$^{\Delta}$β-cell-Ex4.

Effects of exendin-4 on ER stress in Atg7$^{\Delta}$β-cell islets

Based on the close relationship between ER stress and autophagy (22), we also examined the effects of exendin-4 on ER stress markers. First, to assess the state of ER stress, we used electron microscopy (EM) to examine the morphology of ER in β-cells of Atg7$^{f/f}$ and Atg7$^{\Delta\beta\text{-cell}}$ mice treated with or without exendin-4. Atg7$^{\Delta\beta\text{-cell}}$ islets contained dilated ER, considered to be the hallmark of high ER stress, compared with Atg7$^{f/f}$ islets; however, exendin-4 further enhanced ER dilation in the islets (Figure 6A). Analysis of the genes related to unfolded protein response (UPR) showed neither significant changes in the protein expression levels of Bip, phosphorylated PERK/total PERK, phosphorylated eIF2α/total eIF2α, ATF4 and CHOP nor mRNA expression levels of Bip, ATF4, CHOP, and XBP-1 spliced

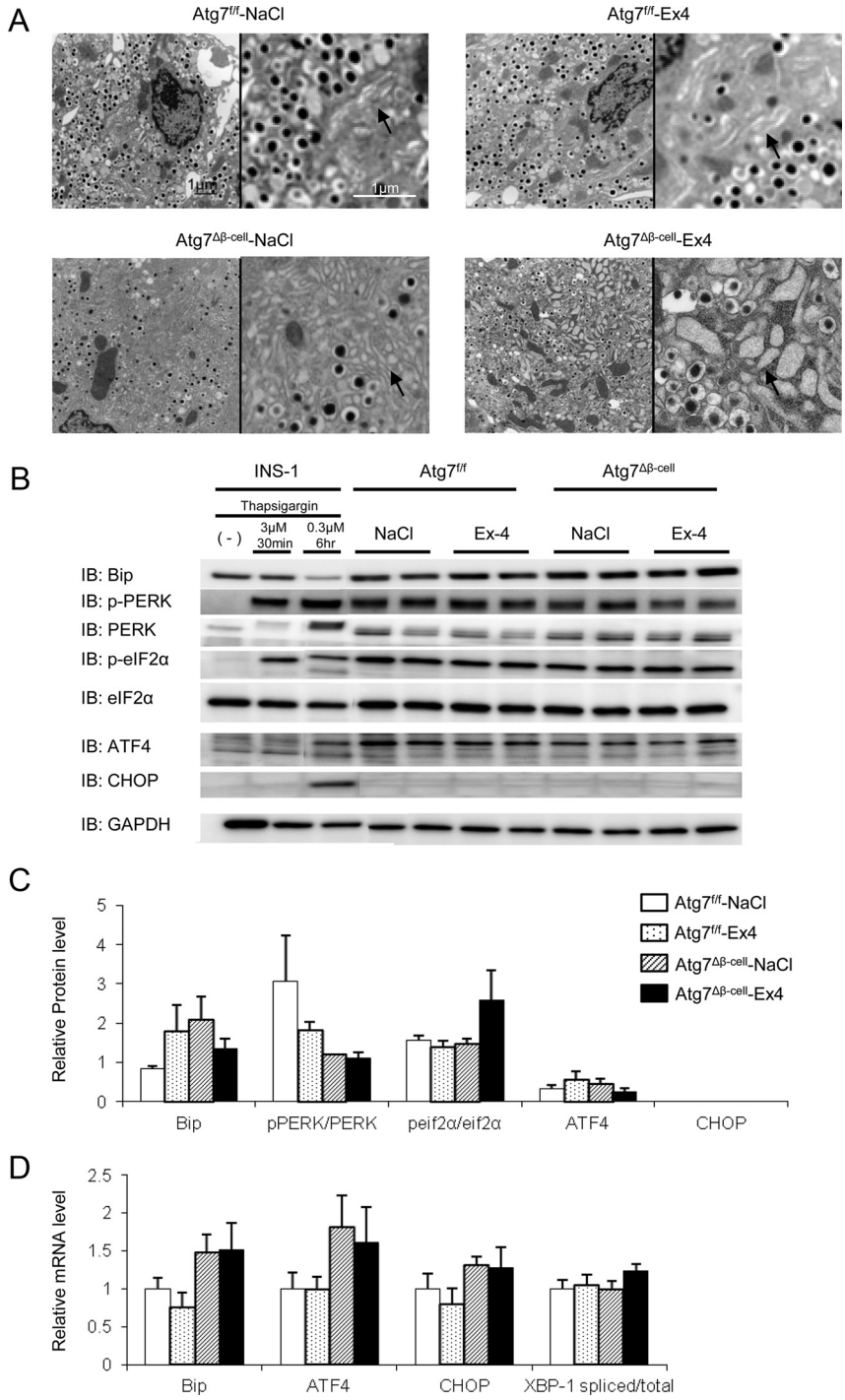

Figure 6. Effects of exendin-4 on morphology of ER and ER stress markers A, Representative images of electron micrographs of Atg7$^{f/f}$-NaCl, Atg7$^{f/f}$-Ex4,Atg7$^{\Delta}\beta$-cell-NaCl, and Atg7$^{\Delta}\beta$-cell-Ex4. Arrows indicated ER. B, Typical protein expression levels in islets isolated from Atg7$^{f/f}$-NaCl, Atg7$^{f/f}$-Ex4, Atg7$^{\Delta}\beta$-cell-NaCl, and Atg7$^{\Delta}\beta$-cell-Ex4. Dimethylsulfoxide-treated INS-1 cells were used as negative control and 2 kinds of thapsigargin-treated (3 μM $\times$ 30 minutes [left lane], 0.3 μM $\times$ 6 hours [right lane]) INS-1 cells were used as weak and strong positive control. C, Quantification of protein expression in each group. Data were obtained from 4 independent experiments. Data are mean $\pm$ SEM. D, The mRNA expression levels in islets of each group. The levels were determined by real-time RT-PCR analysis after extraction of RNA from the isolated islets. Data are mean $\pm$ SEM of 12 independent experiments. Open bars, Atg7$^{f/f}$-NaCl; dotted bars, Atg7$^{f/f}$-Ex4; hatched bars, Atg7$^{\Delta}\beta$-cell-NaCl; solid bars, Atg7$^{\Delta}\beta$-cell-Ex4. GAPDH, glyceraldehydes 3-phosphate dehydrogenase; IB, immunoblotting.

from between Atg7$^{\Delta\beta\text{-cell}}$ islets and Atg7$^{f/f}$ islets (Figure 6, B–D).

Regardless of the expression level of UPR genes, previous data showed diminished survival of ER-stressed islets of Atg7$^{\Delta\beta\text{-cell}}$ mice (18). Thus, we investigated the effects of exendin-4 on cell death of thapsigargin-treated islets. As shown in Figure 7A, increased cell death was evident in islets from Atg7$^{\Delta\beta\text{-cell}}$ mice and exendin-4 reduced thapsigargin-induced cell death to a level comparable to that of Atg7$^{f/f}$ islets. Next, to investigate the effects of exendin-4 in cells with acutely reduced autophagic activity, we established inducible Atg7-gene knock-down system in INS-1 cells based on the expression of small interfering RNA (Atg7KO INS-1). Treatment of such cells with tetracycline for 3 days caused significant suppression of Atg7 expression and accumulation of p62 (Figure 7B). Atg7KD INS-1 cells showed increased cell death, which was enhanced by thapsigargin treatment, and exendin-4 reduced the thapsigargin-induced cell death to a level comparable to that of Atg7WT INS-1 cells (Figure 7C). These results suggest that exendin-4 improves survival of ER-stressed β-cells with autophagy failure.

Discussion

The present study demonstrated accumulation of p62, a representative substrate of autophagy, in islets of *db/db* mice and in type 2 diabetic subjects. These results suggest that failure of autophagy seems to be involved in the pathophysiology of β-cells in patients with type 2 diabetes. With regard to the relationship between autophagy failure and treatment of diabetes, exendin-4, a GLP-1 receptor agonist, improved β-cell function without affecting the expression of p62 in β-cells of *db/db*

mice, We also investigated the mechanism of improvement of autophagy failure-related β-cell dysfunction, by analyzing the effects of exendin-4 on $Atg7^{\Delta\beta\text{-cell}}$ mice. Four-week treatment with exendin-4 improved blood glucose and glucose tolerance in $Atg7^{\Delta\beta\text{-cell}}$ mice mainly by enhancing insulin secretion. Intriguingly, we also found that the same treatment reduced the number of apoptotic cells, increased the number of proliferating cells in islets, and improved survival of ER-stressed islets of $Atg7^{\Delta\beta\text{-cell}}$ mice.

A previous study reported that RIP-Cre mice have mild glucose intolerance (23). However, glucose tolerance in RIP-Cre mice maintained in our facility was similar to that of C57B/L6 mice (24). In addition, glucose tolerance in $Atg7^{f/+}$;RIP-Cre mice was similar to that in $Atg7^{f/f}$ mice (8). For this reason, we used $Atg7^{f/f}$ mice as the control in this study.

Loss of autophagy in β-cells reduces glucose-stimulated insulin secretion and results in inadequate increase in β-cell mass against insulin resistance in mice (8, 9). In a previous study, we showed an increased number of autophagosomes and increased expression level of LC3 type 2 in high-fat-fed C57B/L6 mice and *db/db* mice (8). Furthermore, Masini et al (25) demonstrated the presence of large numbers of autophagosomes and underexpression of lysozymal enzymes, cathepsin B and D, suggesting low autophagic turnover in islets of type 2 diabetes. In agreement with their findings, in the present study we demonstrated accumulation of p62 in islets of *db/db* mice. We also found p62 accumulation in a subset of patients with type 2 diabetes, but not in the control islets, although other markers of autophagic status, such as LC3, and the number of autophagosome could not be assessed in the present study due to lack of sufficient samples (autopsy samples were not well preserved). Recent studies showed that transient exposure to free fatty acids, which are increased in insulin resistance, induces autophagy (26–28), suggesting that transient increase of free fatty acid may enhance, at least in part, autophagy in β-cells to compensate for insulin resistance. On the other hand, another recent study showed that prolonged exposure to free fatty acids impairs autophagic turnover in β-cells (29). Accordingly, lipotoxicity is a potential mechanism of autophagic failure observed in our mouse model of diabetes and patients with type 2 diabetes.

To assess the effect of exendin-4 on β-cell mass, we investigate its effect on apoptotic cell death and the proliferation of β-cells. We found that exendin-4 treatment significantly reduced apoptosis and increased the number of proliferating cells in $Atg7^{\Delta\beta\text{-cell}}$ mice (Figure 5, A–C). However, 4-week treatment did not result in increase of β-cell mass in $Atg7^{\Delta\beta\text{-cell}}$ islets (Figure 5D). It is likely that the treatment period seems to be too short to result in statistically significant increase of

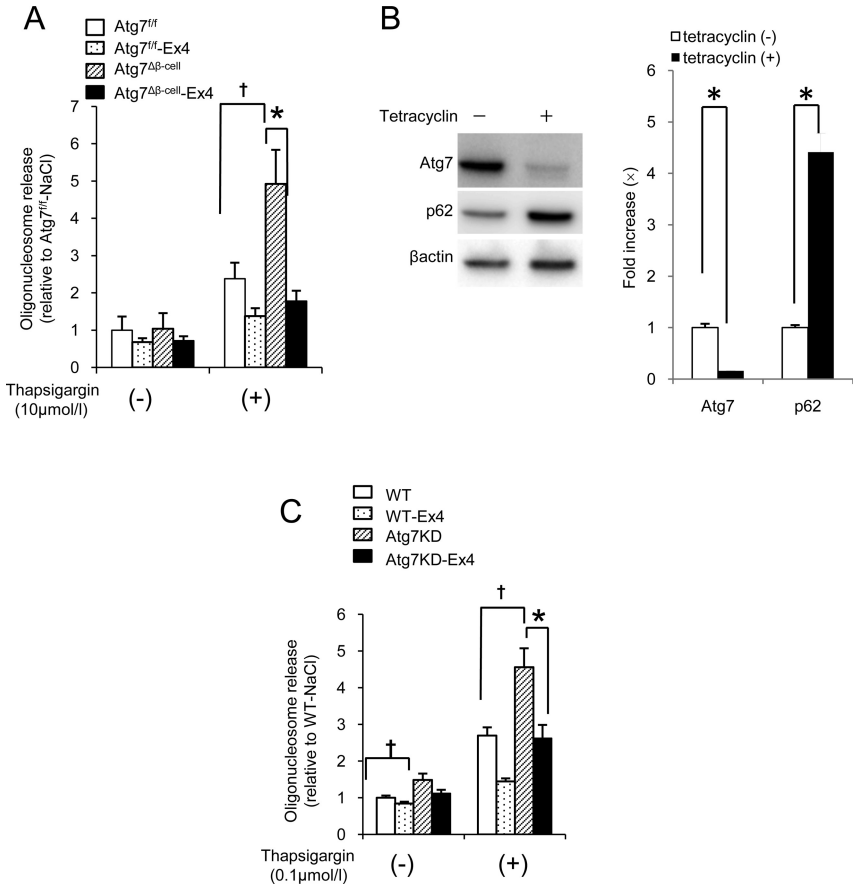

Figure 7. Effects of exendin-4 on cell death associated with ER stress A, Oligonucleosome release from islets isolated from $Atg7^{f/f}$ (open bar, n = 6), $Atg7^{f/f}$ treated with Ex-4 (dotted bar, n = 6), $Atg7^{\Delta}\beta$-cell (hatched bar, n = 5), and $Atg7^{\Delta}\beta$-cell treated with Ex-4 (filled bar, n = 5) with and without thapsigargin. Oligonucleotide release from $Atg7^{f/f}$ without thapsigargin treatment was set at 1.0. *, $P < .01$; $Atg7^{\Delta}\beta$-cell-Ex4 vs $Atg7^{\Delta}\beta$-cell; †, $P < 0.05$; $Atg7^{f/fl}$ vs $Atg7^{\Delta}\beta$-cell. B, Expression of Atg7 and p62 in Atg7WT INS-1 cells and Atg7KD INS-1 cells 72 hours after treatment with tetracycline. Western blotting was performed using Atg7 and p62 antibodies. Representative results (left panel) and quantification of protein expression (right panel). Data are mean ± SEM of 9 independent experiments. *, $P < .01$; vs tetracycline(-). C, Oligonucleosome release from Atg7WT INS-1 (open bar, n = 24), Atg7WT INS-1 treated with Ex-4 (dotted bar, n = 24), Atg7KDINS-1(hatched bar, n = 24), and Atg7KDINS-1 treated with Ex-4 (solid bar, n = 24). *, $P < .01$; Atg7KDINS-1-Ex4 vs Atg7KDINS-1; †, $P < .05$; Atg7KDINS-1 vs WTINS-1. WT, wild type.

β-cell mass. Thus, the improvement in β-cell function of Atg7$^{\Delta\beta\text{-cell}}$ mice following a 4-week exendin-4 treatment seems to be mainly achieved by augmentation of insulin secretion, not by increase in β-cell mass.

GLP-1 receptor agonists activate protein kinase A through the activation of adenylate cyclase. In addition, they activate phosphoinositide 3-kinase, MAPK kinase, and epidermal growth factor receptors. The beneficial effects of GLP-1 receptor agonists on β-cell function are probably mediated through the above complex signaling pathways (30–32). In this study, treatment with exendin-4 produced significant improvement in glucose-stimulated insulin secretion in Atg7$^{\Delta\beta\text{-cell}}$ islets, without affecting ATP level. Although the exact mechanism is unknown, improvement of insulin secretion was associated with increased expression of SNAP25 and synaptotagmine VII in Atg7$^{\Delta\beta\text{-cell}}$ islets. A recent study showed that treatment of *db/db* mice with dipeptidyl peptidase-4 inhibitor increased the expression of SNAP25, an important molecule in exocytosis of insulin-containing granules in β-cell membrane and enhanced glucose-stimulated insulin secretion (33). Although there have been no reports regarding the relation between GLP-1 receptor signal and synaptotagmin VII expression, recent data showed that synaptotagmin VII functions as a positive regulator of insulin secretion and serves as a calcium sensor controlling insulin secretion in pancreatic β-cells (34).Whereas the mechanism and consequence of up-regulation of SNAP25 and synaptotagmine VII should be further elucidated, up-regulation of SNAP25 and synaptotagmin VII may be involved in amelioration of insulin secretion in our model.

Previously, Quan et al (18) reported enhanced thapsigargin-induced cell death and significant underexpression of ER stress markers in Atg7$^{\Delta\beta\text{-cell}}$ islets. Here, Atg7$^{\Delta\beta\text{-cell}}$ islets also showed enhanced-thapsigargin-induced cell death but no changes in the expression of ER stress markers. Although differences in the expression levels of ER stress markers could be due to difference in the age of mice investigated and the food ingredients of the food pellet used in the 2 studies, an important common finding between the present study and the above one is that no substantial increase in the expression of ER stress markers genes was found even under the condition of enhanced ER stress-associated cell death. Thus, our data clearly showed the presence of compromised UPR in Atg7$^{\Delta\beta\text{-cell}}$ islets, in support of the results reported by Quan et al (18).

A previous study demonstrated that exendin-4 modulated UPR and reduced ER stress-associated cell death in cultured β-cell lines and *db/db* mice (35). Although there are no reports on the effects of exendin-4 on survival of β-cells with autophagic failure, intriguingly, exendin-4 abrogated apoptosis of Atg7$^{\Delta\beta\text{-cell}}$ islets and counteracted thapsigargin-induced cell death in Atg7$^{\Delta\beta\text{-cell}}$ islets and Atg7KD INS-1 cells. Amelioration of ER stress-associated cell death by exendin-4 seems to be one of the mechanisms of reduced apoptosis in Atg7$^{\Delta\beta\text{-cell}}$ islets, and it could somehow contribute to the improvement of insulin secretion from Atg7$^{\Delta\beta\text{-cell}}$ islets. However, we found more ER dilation and no substantial changes in expression of ER stress markers in Atg7$^{\Delta\beta\text{-cell}}$ islets treated with exendin-4 .These data suggest that both ER dilation and increased expression of ER stress markers do not simply reflect increased ER stress, especially under the condition of failure of autophagy in islets.

In summary, the results of the present study demonstrated that reduced autophagy in β-cells is common in a mouse model of type 2 diabetes and patients with type 2 diabetes. Although the involved mechanism should be further investigated, our findings suggest that exendin-4 is useful against β-cell dysfunction and increased β-cell apoptosis even in autophagy-deficient β-cells.

Acknowledgments

We thank W. Inaba (Hirosaki University, Hirosaki, Japan), N. Daimaru, E. Magoshi, K. Nakamura, and H. Tsujimura (Juntendo University, Tokyo) for the excellent technical assistance.

Address all correspondence and requests for reprints to: Hirotaka Watada, M.D., Ph.D., or Toyoyoshi Uchida, M.D., Ph.D., Department of Metabolism and Endocrinology, Juntendo University Graduate School of Medicine, 2–1-1 Hongo, Bunkyo-ku, Tokyo 113–8421, Japan. E-mail: hwatada@juntendo.ac.jp or uchitoyo@juntendo.ac.jp.

This work was supported by grants from the Ministry of Education, Sports and Culture of Japan (to H.W. and Y.F.).

Author Contributions: T.U., Y.U., S.Y., Y.F., and H.W. designed the study, analyzed the data and wrote the manuscript. H.A., A.H., H.M., K.K., M.K., N.S., Y.T., and T.O. carried out the experiments, analyzed the data and wrote the manuscript. All authors gave approval of the final version of the manuscript.

Disclosure Summary: Y.F. has received lecture fees from Novartis and Eli Lilly and research funding from MSD and Takeda. H.W. has received lecture fee. from Daiichi Sankyo, Takeda, MSD, Sanofi-Aventis, Ono, Novartis, Astellas, Dainippon Sumitomo, Tanabe Mitsubishi, Novo Nordisk, and Sanwakagaku and research funding from Sanofi-Aventis, Novo Nordisk, Novartis, AstraZeneca, Sanwakagaku, Ono, MSD, Boehringer Ingelheim, Kissei, Takeda, Daiichi Sankyo, and Eli Lilly. All other authors declare no conflict of interest relevant to this manuscript.

References

1. **Rhodes CJ.** Type 2 diabetes-a matter of β-cell life and death? *Science*. 2005;307:380–384.

2. **Ogihara T, Mirmira RG.** An islet in distress: β cell failure in type 2 diabetes. *J Diabetes Invest*. 2010;1:123–133.
3. **Levine B, Klionsky DJ.** Development by self-digestion: molecular mechanisms and biological functions of autophagy. *Dev Cell*. 2004; 6:463–477.
4. **Komatsu M, Waguri S, Chiba T, et al.** Loss of autophagy in the central nervous system causes neurodegeneration in mice. *Nature*. 2006;441:880–884.
5. **Komatsu M, Waguri S, Ueno T, et al.** Impairment of starvation-induced and constitutive autophagy in Atg7-deficient mice. *J Cell Biol*. 2005;169:425–434.
6. **Nakai A, Yamaguchi O, Takeda T, et al.** The role of autophagy in cardiomyocytes in the basal state and in response to hemodynamic stress. *Nat Med*. 2007;13:619–624.
7. **Hara T, Nakamura K, Matsui M, et al.** Suppression of basal autophagy in neural cells causes neurodegenerative disease in mice. *Nature*. 2006;441:885–889.
8. **Ebato C, Uchida T, Arakawa M, et al.** Autophagy is important in islet homeostasis and compensatory increase of β cell mass in response to high-fat diet. *Cell Metab*. 2008;8:325–332.
9. **Jung HS, Chung KW, Won Kim J, et al.** Loss of autophagy diminishes pancreatic β cell mass and function with resultant hyperglycemia. *Cell Metab*. 2008;8:318–324.
10. **Wu JJ, Quijano C, Chen E, et al.** Mitochondrial dysfunction and oxidative stress mediate the physiological impairment induced by the disruption of autophagy. *Aging*. 2009;1:425–437.
11. **Kaku K, Rasmussen MF, Nishida T, Seino Y.** Fifty-two-week, randomized, multicenter trial to compare the safety and efficacy of the novel glucagon-like peptide-1 analog liraglutide vs glibenclamide in patients with type 2 diabetes. *J Diabetes Invest*. 2011;2:441–447.
12. **Inagaki N, Ueki K, Yamamura A, Saito H, Imaoka T.** Long-term safety and efficacy of exenatide twice daily in Japanese patients with suboptimally controlled type 2 diabetes. *J Diabetes Invest*. 2011;2: 448–456.
13. **Onishi Y, Koshiyama H, Imaoka T, Haber H, Scism-Bacon J, Boardman MK.** Safety of exenatide once weekly for 52 weeks in Japanese patients with type 2 diabetes mellitus. *J Diabetes Invest*. 2013;4:182–189.
14. **Li Y, Hansotia T, Yusta B, Ris F, Halban PA, Drucker DJ.** Glucagon-like peptide-1 receptor signaling modulates β cell apoptosis. *J Biol Chem*. 2003;278:471–478.
15. **Stoffers DA, Kieffer TJ, Hussain MA, et al.** Insulinotropic glucagon-like peptide 1 agonists stimulate expression of homeodomain protein IDX-1 and increase islet size in mouse pancreas. *Diabetes*. 2000; 49:741–748.
16. **Park S, Dong X, Fisher TL, et al.** Exendin-4 uses Irs2 signaling to mediate pancreatic β cell growth and function. *J Biol Chem*. 2006; 281:1159–1168.
17. **Uchida T, Iwashita N, Ohara-Imaizumi M, et al.** Protein kinase Cδ plays a non-redundant role in insulin secretion in pancreatic β cells. *J Biol Chem*. 2007;282:2707–2716.
18. **Quan W, Hur KY, Lim Y, et al.** Autophagy deficiency in β cells leads to compromised unfolded protein response and progression from obesity to diabetes in mice. *Diabetologia*. 2012;55:392–403.
19. **Nakayama S, Arakawa M, Uchida T, et al.** Dose-dependent requirement of patched homologue 1 in mouse pancreatic β cell mass. *Diabetologia*. 2008;51:1883–1892.
20. **Shimoda M, Kanda Y, Hamamoto S, et al.** The human glucagon-like peptide-1 analogue liraglutide preserves pancreatic β cells via regulation of cell kinetics and suppression of oxidative and endoplasmic reticulum stress in a mouse model of diabetes. *Diabetologia*. 2011; 54:1098–1108.
21. **Arakawa M, Ebato C, Mita T, et al.** Effects of exendin-4 on glucose tolerance, insulin secretion, and β-cell proliferation depend on treatment dose, treatment duration and meal contents. *Biochem Biophys Res Commun*. 2009;390:809–814.
22. **Yin JJ, Li YB, Wang Y, et al.** The role of autophagy in endoplasmic reticulum stress-induced pancreatic β cell death. *Autophagy*. 2012; 8:158–164.
23. **Lee JY, Ristow M, Lin X, White MF, Magnuson MA, Hennighausen L.** RIP-Cre revisited, evidence for impairments of pancreatic β-cell function. *J Biol Chem*. 2006;281:2649–2653.
24. **Iwashita N, Uchida T, Choi JB, et al.** Impaired insulin secretion in vivo but enhanced insulin secretion from isolated islets in pancreatic β cell-specific vascular endothelial growth factor-A knock-out mice. *Diabetologia*. 2007;50:380–389.
25. **Masini M, Bugliani M, Lupi R, et al.** Autophagy in human type 2 diabetes pancreatic β cells. *Diabetologia*. 2009;52:1083–1086.
26. **Martino L, Masini M, Novelli M, et al.** Palmitate activates autophagy in INS-1E β-cells and in isolated rat and human pancreatic islets. *PloS one*. 2012;7:e36188.
27. **Komiya K, Uchida T, Ueno T, et al.** Free fatty acids stimulate autophagy in pancreatic β-cells via JNK pathway. *Biochem Biophys Res Commun*. 2010;401:561–567.
28. **Tan SH, Shui G, Zhou J, et al.** Induction of autophagy by palmitic acid via protein kinase C-mediated signaling pathway independent of mTOR (mammalian target of rapamycin). *J Biol Chem*. 2012; 287:14364–14376.
29. **Las G, Serada SB, Wikstrom JD, Twig G, Shirihai OS.** Fatty acids suppress autophagic turnover in β-cells. *J Biol Chem*. 2011;286: 42534–42544.
30. **Wang Q, Li L, Xu E, Wong V, Rhodes C, Brubaker PL.** Glucagon-like peptide-1 regulates proliferation and apoptosis via activation of protein kinase B in pancreatic INS-1 β cells. *Diabetologia*. 2004; 47:478–487.
31. **Li L, El-Kholy W, Rhodes CJ, Brubaker PL.** Glucagon-like peptide-1 protects β cells from cytokine-induced apoptosis and necrosis: role of protein kinase B. *Diabetologia*. 2005;48:1339–1349.
32. **Kwon G, Pappan KL, Marshall CA, Schaffer JE, McDaniel ML.** cAMP Dose-dependently prevents palmitate-induced apoptosis by both protein kinase A- and cAMP-guanine nucleotide exchange factor-dependent pathways in β-cells. *J Biol Chem*. 2004;279:8938–8945.
33. **Nagamatsu S, Ohara-Imaizumi M, Nakamichi Y, Aoyagi K, Nishiwaki C.** DPP-4 inhibitor des-F-sitagliptin treatment increased insulin exocytosis from db/db mice β cells. *Biochem Biophys Res Commun*. 2011;412:556–560.
34. **Gustavsson N, Lao Y, Maximov A, et al.** Impaired insulin secretion and glucose intolerance in synaptotagmin-7 null mutant mice. *Proc Natl Acad Sci USA*. 2008;105:3992–3997.
35. **Yusta B, Baggio LL, Estall JL, et al.** GLP-1 receptor activation improves β cell function and survival following induction of endoplasmic reticulum stress. *Cell Metab*. 2006;4:391–406.